

# Application of Two-Dimensional Correlation Infrared Spectroscopy to the Study of Miscible Polymer Blends

He Huang, Serghei Malkov, Michael Coleman, and Paul Painter\*

Department of Materials Science and Engineering, Pennsylvania State University, University Park, Pennsylvania 16802

Received December 11, 2002; Revised Manuscript Received May 21, 2003

**ABSTRACT:** In the preceding paper in this series, generalized two-dimensional (2D) correlation vibrational spectroscopy was applied to the study of immiscible polymer blends. Here miscible systems are considered. It is shown that new features that appear in 2D plots that were previously interpreted in terms of bands that can be associated with specific interactions or conformational changes are artifacts of the procedure used to obtain these plots. The features actually correspond to "lobes" or points of inflection in the difference spectra used to generate the 2D plots that are a result of small frequency shifts or bandwidth changes.

## Introduction

In the first paper<sup>1</sup> of this series, where we are systematically studying the application of correlation infrared spectroscopy to the characterization of polymer blends, we examined synchronous and asynchronous two-dimensional plots, generated from a series of infrared spectra obtained as a function of blend composition. We examined normalization methodologies and discussed how bandwidth changes can lead to readily recognizable patterns in the plots. Here we will continue our studies by considering two miscible systems with relatively weak intermolecular interactions: blends of atactic polystyrene (PS) with poly(2,6-dimethyl-1,4-phenylene ether) (PPO) and blends of polystyrene (PS) with poly(vinyl methyl ether) (PVME). Both of these systems have been studied by traditional "linear" infrared spectroscopy<sup>2–5</sup> and by 2D infrared spectroscopy.<sup>6,7</sup> Satkowsky et al.<sup>7</sup> used dynamic infrared linear dichroism in their study of the deuterated d-PS/PVME system, while Nakashima et al.<sup>6</sup> studied PS/PPO blends as a function of concentration using correlation spectroscopy in the mid-infrared region. It is this latter work that will concern us here.

Earlier work on PS/PVME blends<sup>3–5</sup> demonstrated that bands associated with the CH out-of-plane bending mode of PS and the COCH<sub>3</sub> group of PVME were perturbed upon forming miscible blends, while aromatic ring modes were sensitive to mixing in PS/PPO blends.<sup>2</sup> In this latter system, bands associated with the aromatic ether stretching mode also showed significant changes, and this was interpreted in terms of conformational changes. Nakashima et al.<sup>6</sup> identified a previously undetected band in this region of the spectrum using correlation infrared spectroscopy and also bands in other regions of the spectra that are difficult to detect with conventional methods.

These are potentially exciting results and should make this method a powerful tool for studying interactions in many systems. Unfortunately, as we will show here, the new features generated in the two-dimensional asynchronous plots are usually a result of small frequency shifts and/or bandwidth changes in modes that

are clearly visible in the original spectra and are not a result of revealing underlying, difficult to detect new bands.

## Experimental Section

The polymer samples used in this study are listed in Table 1. Sample preparation techniques and calculation methodologies are as described in the preceding paper.<sup>1</sup>

## Results and Discussion

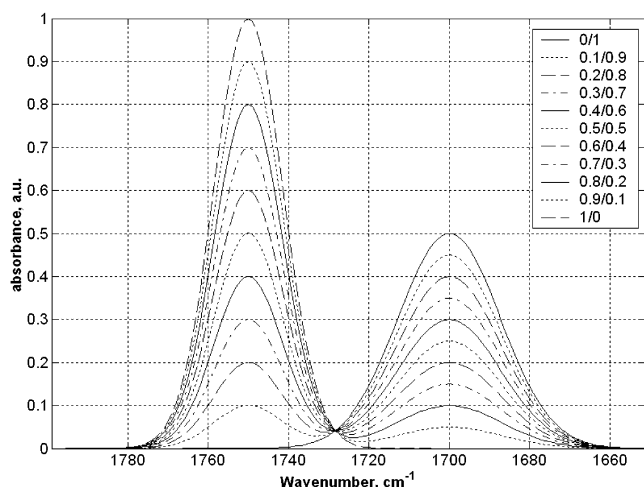
To interpret the plots obtained using correlation infrared spectroscopy to characterize "weak" interactions in polymer blends, we will need to be familiar with the effect of bandwidth changes and frequency shifts. We discussed the former in the preceding paper<sup>1</sup> and demonstrated how it gave rise to a (45° rotated) four-leaf clover like pattern, as discussed in previous work.<sup>8–12</sup> In this paper we will start by considering a simulation to illustrate the complexity of what can be observed. We synthesized two bands, such that each represents a separate component of a blend. The intensity of each was varied in a linear fashion with concentration (and so varied inversely with one another), as shown in Figure 1. Figure 2 displays the synchronous and asynchronous contour plots obtained from these spectra (after mean normalization; see preceding paper). The synchronous spectra are as we would expect them to be, displaying two peaks on the diagonal corresponding to the bands in the original infrared spectra and two off-diagonal peaks whose intensities are negative (shaded), indicating that the intensities of these two bands giving rise to these plots vary inversely with one another.

If the bands in the original spectra vary in a simple linear fashion with concentration, then we should not be able to calculate asynchronous spectra (one simply gets noise). However, we allowed the bandwidth at half-height of the two bands to vary slightly with composition, 0.01 and 0.05 cm<sup>-1</sup> per increment (or decrement) of concentration (the initial bandwidths were set to 20 and 30 cm<sup>-1</sup>, respectively). The total change of bandwidth is small, 0.1 and 0.5 cm<sup>-1</sup>, respectively, but the effect on the asynchronous spectrum is quite startling. The diagonal peaks observed in the synchronous plot are each split into the rotated four-leaf clover like pattern.

\* To whom correspondence should be addressed.

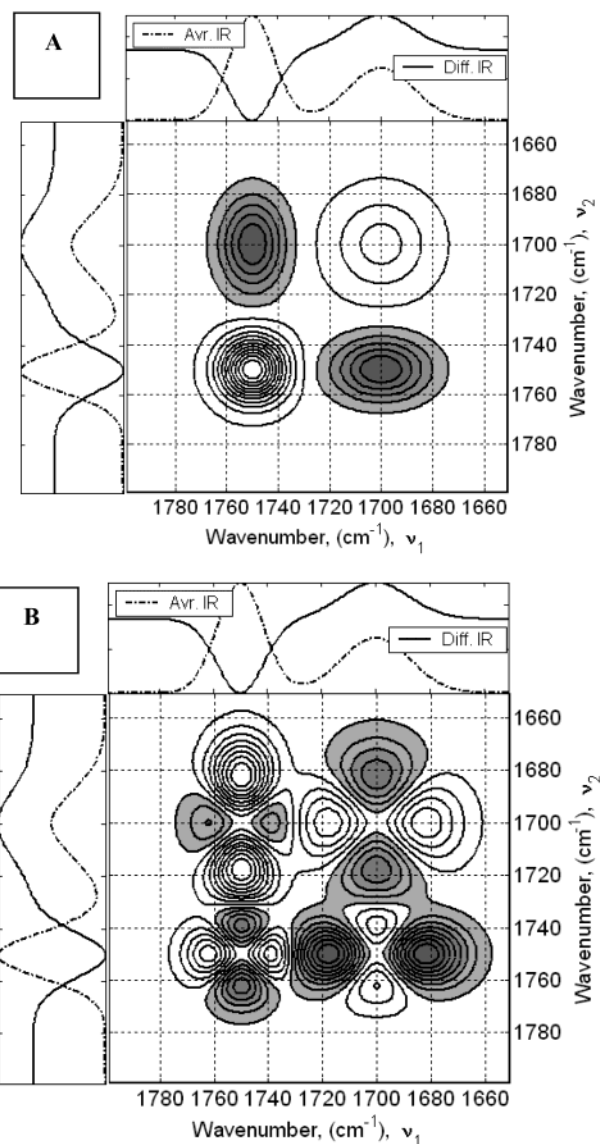
**Table 1. Polymer Samples and Their Molecular Weights**

| name                                   | abbreviation | MW <sup>a</sup>  | source                             |
|--|--------------|------------------|------------------------------------|
| polystyrene                            | PS           | $M_w = 190\,000$ | Scientific Polymer Production Inc. |
| poly(vinyl methyl ether)               | PVME         | $M_w = 90\,000$  | Scientific Polymer Production Inc. |
| poly(2,6-dimethyl-1,4-phenylene oxide) | PPO          | $M_w = 50\,000$  | Scientific Polymer Production Inc. |

<sup>a</sup> Weight-average.**Figure 1.** Simulated IR spectra of two bands centered at  $1750\text{ cm}^{-1}$  ( $w_{1/2} = 20\text{ cm}^{-1}$ ) and  $1700\text{ cm}^{-1}$  ( $w_{1/2} = 30\text{ cm}^{-1}$ ) with a bandwidth change of  $0.01$  and  $0.05\text{ cm}^{-1}$  per increment (decrement), respectively.

This result is easily understood if one recalls the methodology used to obtain these plots (see preceding paper). Essentially, a mean spectrum is obtained, and this is subtracted from the other spectra in the sample set. Subtracting a narrow band from a broad one results in two positive lobes on each side of a negative band or, depending on relative intensities, two points of inflection on each side of a negative lobe. This pattern is reversed when a broad band is subtracted from a narrow band. It is these lobes or points of inflection that give rise to the asynchronous peaks in the subsequent correlation analysis.

Small frequency shifts have an equally pronounced effect on the spectra, as demonstrated in other studies.<sup>8–12</sup> To illustrate this, we again considered two bands, each of those intensity varied linearly with concentration. This time we allowed the wavenumber of each mode to shift  $0.05$  and  $0.01\text{ cm}^{-1}$  per concentration increment (for a total shift of  $0.5$  and  $0.1\text{ cm}^{-1}$  over the concentration range of these simulated spectra, respectively). Figure 3 shows the synchronous and asynchronous plots obtained from these spectra. Once more, the synchronous plots are as expected, but band shifts result in the appearance of asynchronous peaks. Again, the asynchronous bands correspond to peaks appearing in the synchronous plots, but each is split into two components around a diagonal. One of the “split” components is always positive while the other is always negative, a reflection of the direction of the frequency shift of the bands in the original infrared spectra. As before, these asynchronous peaks have their origin in the difference spectra used to generate the plots. Subtracting one band from another when the two are shifted, a small amount results in the presence of negative and positive difference bands, each somewhat shifted from the positions of the original modes. It is these difference bands that give rise to the asynchronous

**Figure 2.** Synchronous (A) and asynchronous (B) contour plots of “synthetic” IR spectra of the two bands centered at  $1750$  and  $1700\text{ cm}^{-1}$  shown in Figure 1.

peaks. We will demonstrate this directly in the spectra of “real” systems later in this paper.

One problem in using simulated spectra pointed out to us by one of the reviewers of this paper is that there can be an effect due to noise in real systems that is neglected in such studies. However, our goal in using such simulations is simply to demonstrate the type of patterns one would expect to see. The asynchronous pattern actually stays the same when random noise is added, but the features or bands in the contour plot each become more or less systematically distorted around the original positions as a result of noise. This is shown in Figure 4, where  $0.1\%$  noise has been added to the spectra used to obtain Figure 3. The spectra of “real” systems we will turn to now

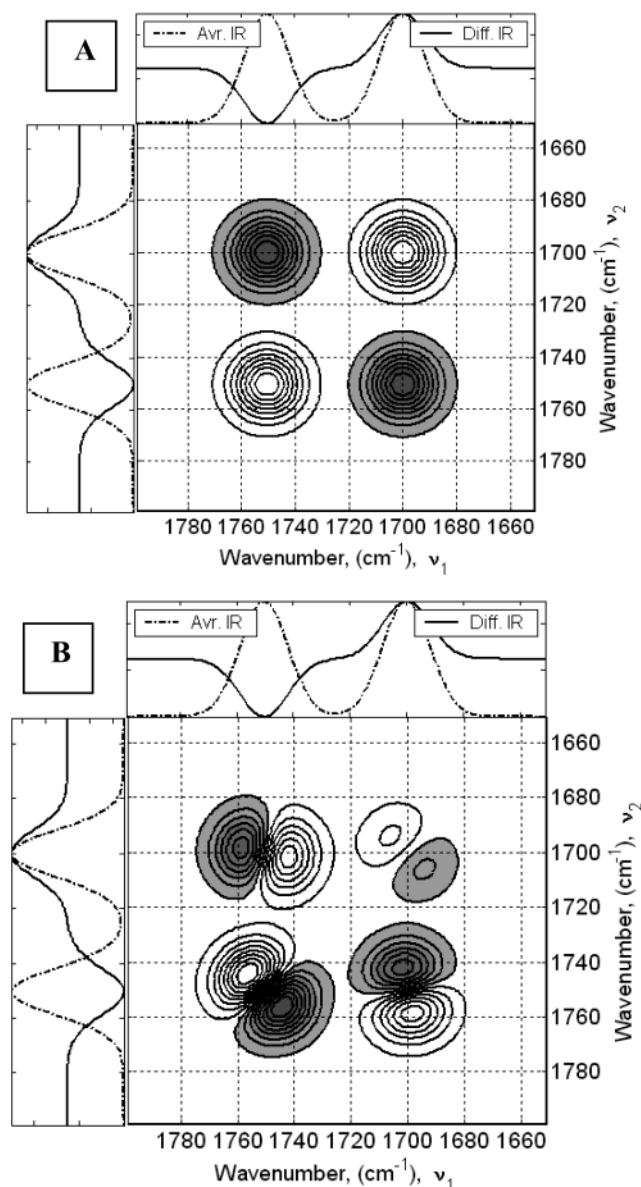


**Figure 3.** Synchronous (A) and asynchronous (B) contour plots of “synthetic” IR spectra of two bands centered at 1750 and 1700  $\text{cm}^{-1}$  (bandwidth = 20  $\text{cm}^{-1}$ ), each with a peak shift of 0.05 and 0.01  $\text{cm}^{-1}$  per increment (decrement), respectively.

have a high signal-to-noise ratio and do not show such distortions.

An example of the effect of frequency shifts in a blend of PS with PVME is shown in Figure 5. Following Nakashima et al.,<sup>6</sup> we split our blend samples into two sets: one with high concentrations of PS (PS/PVME; 90/10, 80/20, 70/30, 60/40) and the other with high concentrations of PVME (PS/PVME; 40/60, 30/70, 20/80, 10/90). In blends with high PVME concentrations, the effect of interactions on PS bands should be maximized, and vice versa. Figure 5 shows plots obtained in the aromatic CH stretching region (3100–3000  $\text{cm}^{-1}$ ) for the high PVME content blends. It can be seen that all of the bands that appear in the synchronous spectra appear in the asynchronous plots, but each is split around a diagonal running through the center of the original synchronous band. Clearly, we are not detecting new bands but simply the effect of band shifts. The problem is trying to ascertain whether these shifts are due to interactions or due to refractive index changes,

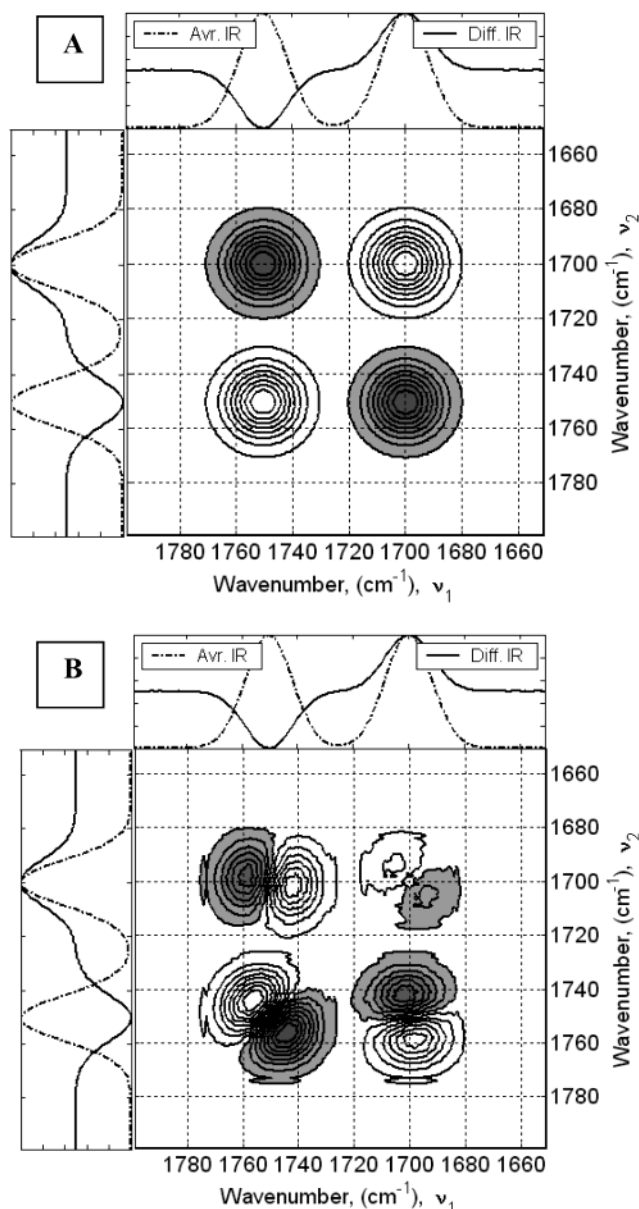


**Figure 4.** Synchronous (A) and asynchronous (B) contour plots of “synthetic” IR spectra of two bands centered at 1750 and 1700  $\text{cm}^{-1}$  (bandwidth = 20  $\text{cm}^{-1}$ ), shown in Figure 3, with random noise of 0.1%.

sample preparation problems (that lead to reflections, wedge effects, etc.; see preceding paper), and so on.

The answer in this system is probably all of the above. If we compare the plots obtained from the miscible PS/PVME system to plots obtained from the infrared spectra of immiscible PS/PMMA blends (at equivalent concentrations), shown in Figure 6, it can be seen that splittings are also obtained. In this latter case the split components are more tightly clustered around the diagonal separating them, indicating smaller frequency shifts. These small frequency shifts and/or bandwidth changes can actually be observed in the original, scale-expanded spectra, as shown in Figure 7. It is reasonable to assume that the larger frequency shifts that can be observed in the miscible PS/PVME blends are then probably a result of the PS chains experiencing a difference in local environment (in addition to any shifts that can be attributed to refractive index changes, etc.). But such small shifts are, in our view, unlikely to be



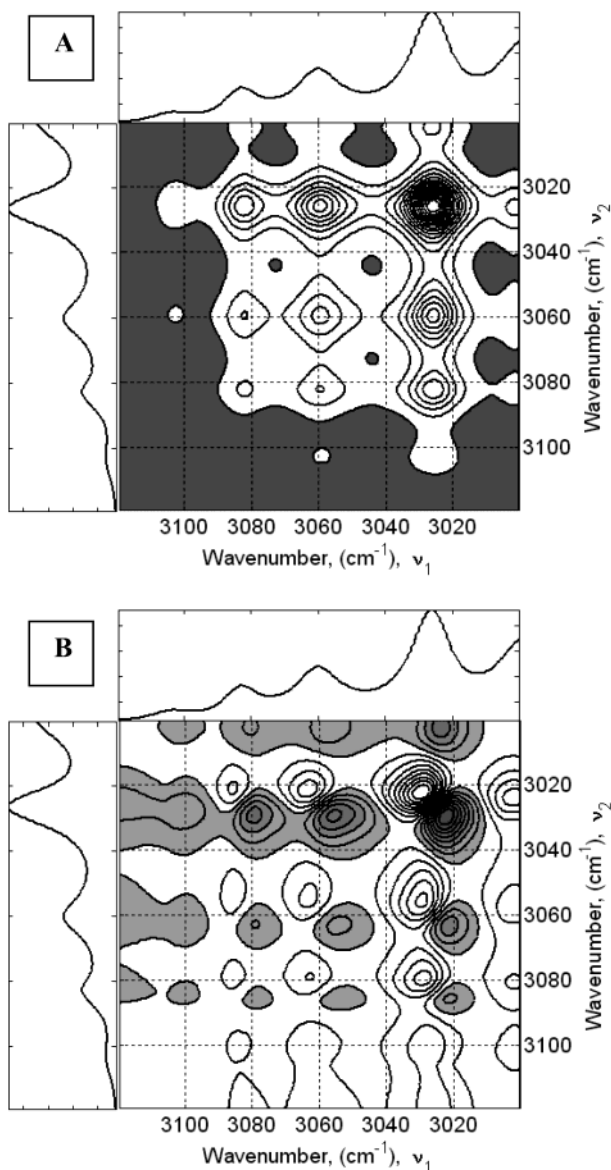


**Figure 5.** Synchronous (A) and asynchronous (B) contour plots of PS/PVME blends with high PVME (see text) content in the C–H stretching region of 3120–3000  $\text{cm}^{-1}$ . The spectra were first mean normalized.

attributable to the type of interaction that could drive miscibility in these types of blends (i.e., where the presence of strong, specific interactions is not obvious).

Given these results, we believe work previously reported in the literature needs to be reinterpreted. For example, Nakashima et al.<sup>6</sup> obtained synchronous and asynchronous plots in the 1600  $\text{cm}^{-1}$  region of the spectra of PS/PPO blends. We repeated this work and obtained similar results, shown in parts A and B of Figure 8 for high PS and low PS content blends, respectively. These figures only show asynchronous spectra. The synchronous plots are as reported by Nakashima et al. and are as one would expect.

In both plots it can be seen that there is a cloverleaf-like pattern, centered near 1600  $\text{cm}^{-1}$ , as also observed by Nakashima et al. In our plots there is also a “smearing” of intensity at the top and right-hand edges, respectively. This is because we did not adjust our baselines in this local region of the spectra. Furthermore, the intensity patterns on the leaves of our “clover” are reversed (relative to the result of Nakashima et al.).

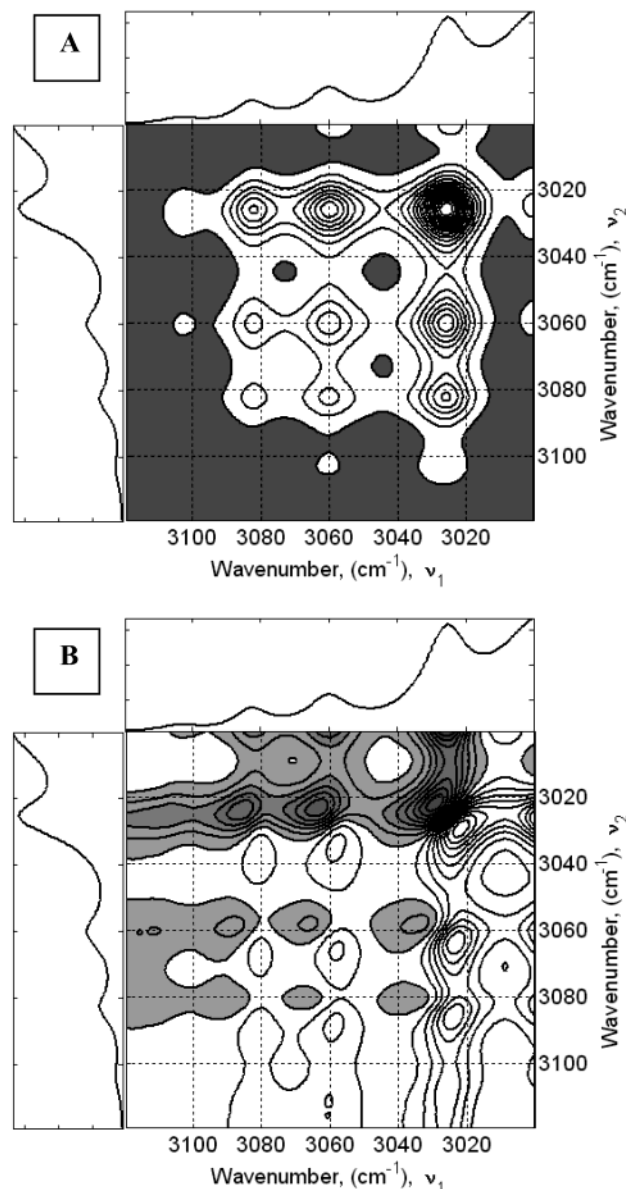


**Figure 6.** Synchronous (A) and asynchronous (B) contour plots of PS/PMMA blends with high PMMA content in the C–H stretching region of 3120–3000  $\text{cm}^{-1}$ . The spectra were first mean normalized.

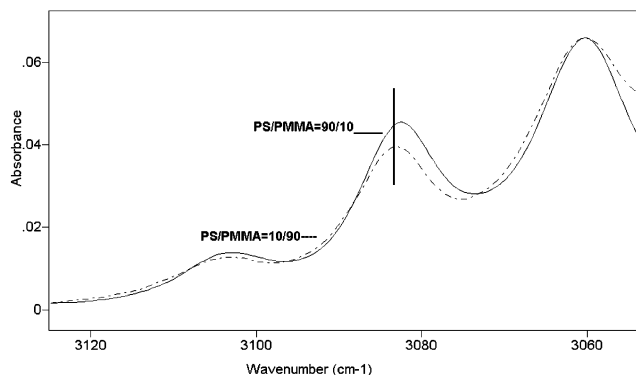


**Figure 7.** Scale-expanded spectra of PS/PMMA = 90/10 and PS/PMMA = 10/90 in the region of 3120–3050  $\text{cm}^{-1}$ .

In Figure 8A, positive intensity lobes are obtained on the top and bottom (unshaded) and negative intensity lobes (shaded) to the right and left. This pattern is reversed in Figure 8B. However, this pattern is merely

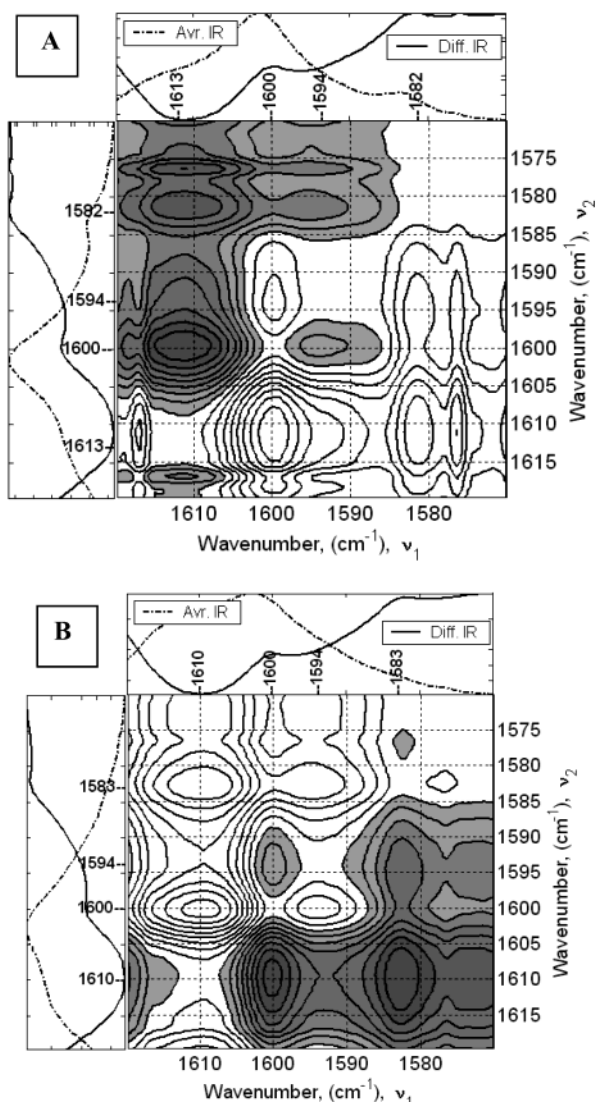


**Figure 8.** Asynchronous contour plots of PS/PPO blends in the region of 1630–1570  $\text{cm}^{-1}$  with high (A) or low (B) PS content.

a reflection of the order in which the spectra are incorporated into the correlation analysis. In one order (decreasing PS content) a broader profile is being subtracted from a narrower one, while this reversed if the spectra are incorporated in the opposite (concentration) direction (i.e., increasing PS content).

Clearly, this pattern is identical to the one obtained when bands are changing their half-width. Here, however, we have bands from both PS and PPO contributing to the overall spectral profile, which is changing with composition. Nevertheless, the effect is the same. Also shown on the top and side of Figure 8A,B are the “mean” infrared spectra (sum of the spectra of all four blends divided by four) and the difference spectrum obtained by subtracting this mean spectrum from the highest PS content blend in each sample set (90/10 and 40/60, respectively). A typical scale-expanded difference spectrum and its second derivative are shown in Figure 9. Clearly, the contour peak maxima and minima correspond to “concave upward” and “concave downward” lobes in the difference spectra, which are changing in a nonlinear fashion with concentration, thus giving rise to corresponding bands in the asynchronous plot. In other words, it is not only a change in the breadth of a

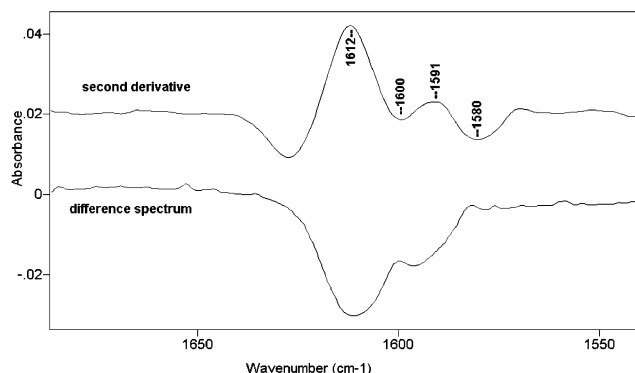


**Figure 9.** Difference spectrum of PS/PPO = 90/10 and its second derivative in the region of 1700–1530  $\text{cm}^{-1}$ .

single band that can give rise to such patterns in asynchronous spectra but also changes in overall band profiles. These spectra have previously been interpreted in terms of the presence of bands at 1614, 1601, 1594, and 1583  $\text{cm}^{-1}$ . The “order” of intensity changes, based on which bands are positive and negative in the synchronous and asynchronous plots, following Noda,<sup>13</sup> were then interpreted in terms of specific interactions in the blends. We believe this is erroneous because in this case the features in the 2-D plots correspond to difference bands generated by profile changes, not the fundamental normal modes themselves. This also explains why it has often been observed that bands in correlation plots are shifted from the position of bands in the original spectra. It is simply a result of the fact that difference spectra are used to obtain correlation plots, and it is the “upward” and “downward” pointing lobes or points of inflection in these difference spectra that give rise to peaks in asynchronous plots.

Other features in asynchronous plots have been similarly misinterpreted. For example, if we turn our attention to the 1200  $\text{cm}^{-1}$  region of the spectra of PS/PPO blends, where a strong band or bands associated with the aromatic C–O–C ether stretching mode appears, then the asynchronous plots shown in Figure 10A,B are obtained. These plots are similar to those obtained by Nakashima et al.,<sup>6</sup> displaying the rotated cloverleaf pattern, although in the asynchronous plots of the high PS content blends this pattern is less pronounced, a point we will return to shortly. Nakashima et al.<sup>6</sup> interpreted these peaks in terms of the presence of three bands in the original infrared spectra and made the point that the lowest frequency one (near 1176  $\text{cm}^{-1}$ ) could not be identified by conventional “one-dimensional” infrared spectroscopy. Each of the three bands was then assigned to a particular configuration. However, if the difference spectra obtained from the low PS content blends, for example, are carefully examined, then it is clear that these bands appear to correspond to lobes or points of inflection in the difference spectra.

We were stuck by the fact that two of the “leaves” of our cloverleaf pattern in high PS content blends are relatively weak. These lobes are much stronger in the plots reported by Nakashima et al.,<sup>6</sup> but these authors used a different number of blends to obtain their correlation plots and cast films from a different solvent. To compare our results directly, we did not mean normalize our spectra before analysis (see preceding paper). Mean normalization largely removes two of the lobes, giving the asynchronous plot shown in Figure 11. This pattern is strikingly similar to that obtained from

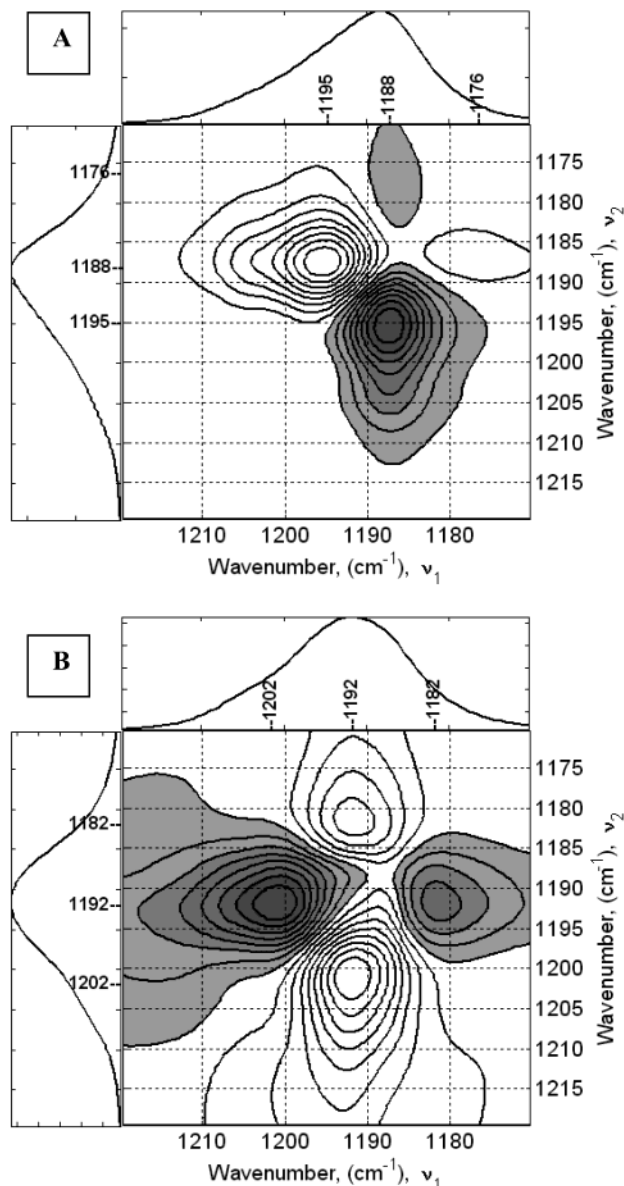


**Figure 10.** Asynchronous contour plots of PS/PPO blends in the region of 1220–1170  $\text{cm}^{-1}$  with high (A) or low (B) PS content.

blends that shift in frequency but could also be a result of the presence of two bands that are changing relative to one another and in a nonlinear fashion with concentration (note that the band near 1180  $\text{cm}^{-1}$  observed by Nakashima et al. is no longer apparent).

The origin of the apparent frequency shift and an interpretation of what is occurring are more easily obtained from conventional “linear” infrared spectroscopy. Figure 12 compares the 1200  $\text{cm}^{-1}$  region of the spectra of a 90/10 PS/PPO composition blend to that of a 60/40 blend. The band profile is indeed shifted. Furthermore, the band profile can be curve resolved into just two components, as shown in Figure 13 (for the PS/PPO 90/10 blend). There is no need to include an additional band near 1180  $\text{cm}^{-1}$  to obtain a good fit. Clearly, it is dangerous to simply apply correlation analysis without a careful study of the original spectra.

So far, the results we have discussed have proved disappointingly negative. The bands observed in the asynchronous spectra are due to features in difference spectra that are a result of frequency shifts and/or

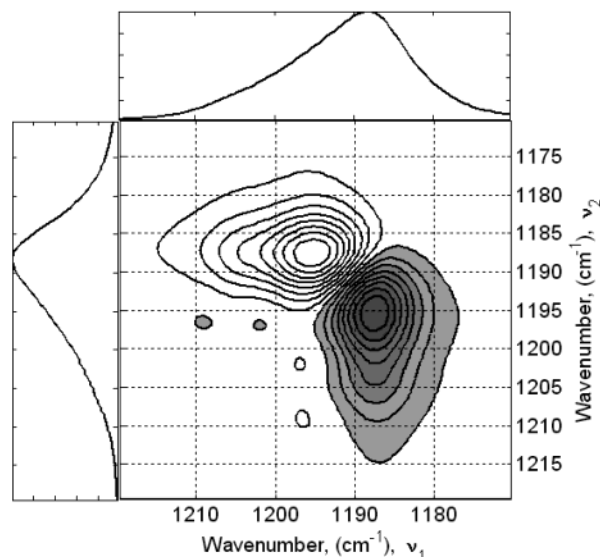


**Figure 11.** Asynchronous contour plots of PS/PPO blends with high PS content in the region of 1220–1170  $\text{cm}^{-1}$ . The spectra were first mean normalized.

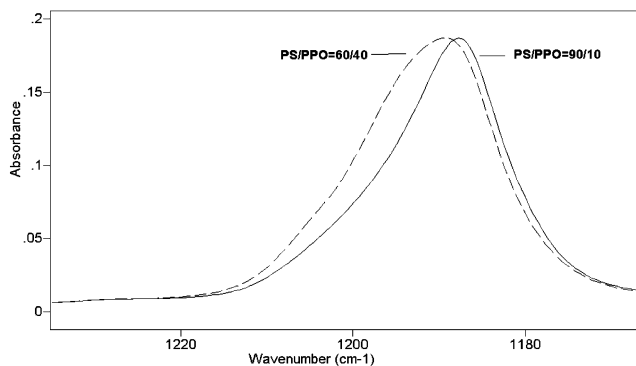


**Figure 12.** IR spectra of PS/PPO = 90/10 and 60/40 blends around 1200  $\text{cm}^{-1}$ .

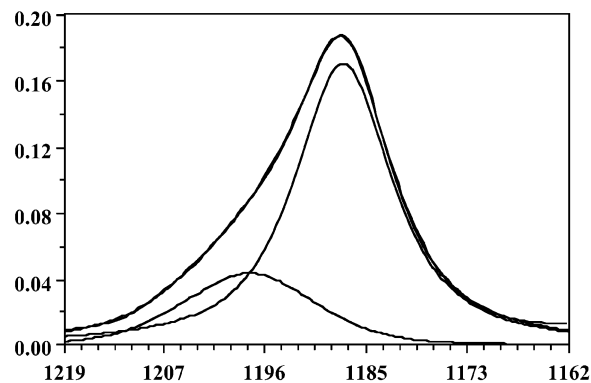


**Figure 13.** Result of curve fitting the band around 1190  $\text{cm}^{-1}$  for a PS/PPO = 90/10 blend.

bandwidth changes. These can have their origin in sample preparation effects, small changes in refractive index, etc., in addition to any effect due to interactions or conformational changes. However, we have focused our attention on the PS/PPO system, which under the sample preparation conditions used here, chosen so as to reproduce the results reported in the literature, is complicated by the possibility of crystallization of the PPO component. Accordingly, we also studied PS/PVME blends, as neither component of this mixture of atactic polymers is capable of crystallizing. In many regions of



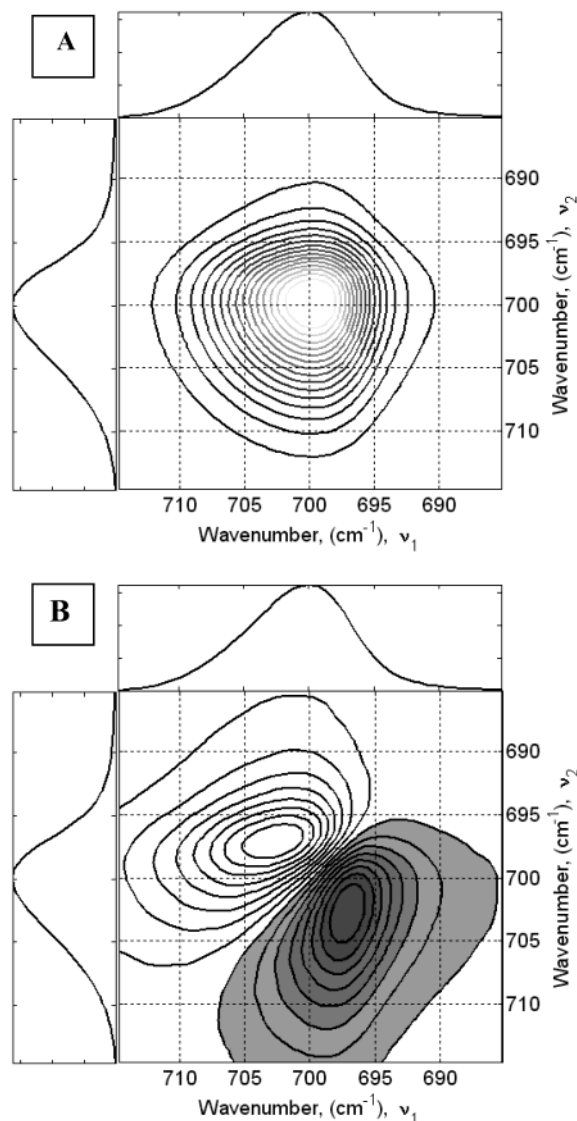


**Figure 14.** Synchronous (A) and asynchronous (B) contour plots of PS/PVME blends with high PVME content in the C–H out-of-plane bending mode region (715–685  $\text{cm}^{-1}$ ) of PS.

the spectra (CH stretching, 1600  $\text{cm}^{-1}$  ring breathing mode, etc.), we found similar patterns to those observed in immiscible PS/PMMA blends or PS/PPO blends, features in the contour plots that upon careful examination of the difference spectra could be assigned to small frequency shifts and/or small bandwidth changes. As mentioned above, such small changes are not definitive, in that they can have their origin in effects other than specific interactions. Two regions of the spectra gave results that are worth commenting on, however.

The first of these is the 700  $\text{cm}^{-1}$  region, where there is very strong absorbance due to the aromatic CH out-of-plane bending mode of polystyrene. Synchronous and asynchronous contour plots, obtained from high PVME content blends, are shown in Figure 14. Although there are two bands contributing to this profile that are readily discerned by eye and in the second derivative of the spectrum, their frequencies are too close to be revealed in the synchronous plot. The asynchronous spectra form a pattern that is characteristic of a frequency shift, but one that is much larger than in the spectra of PS/PMMA and PS/PPO blends. This shift can also be seen in the original infrared

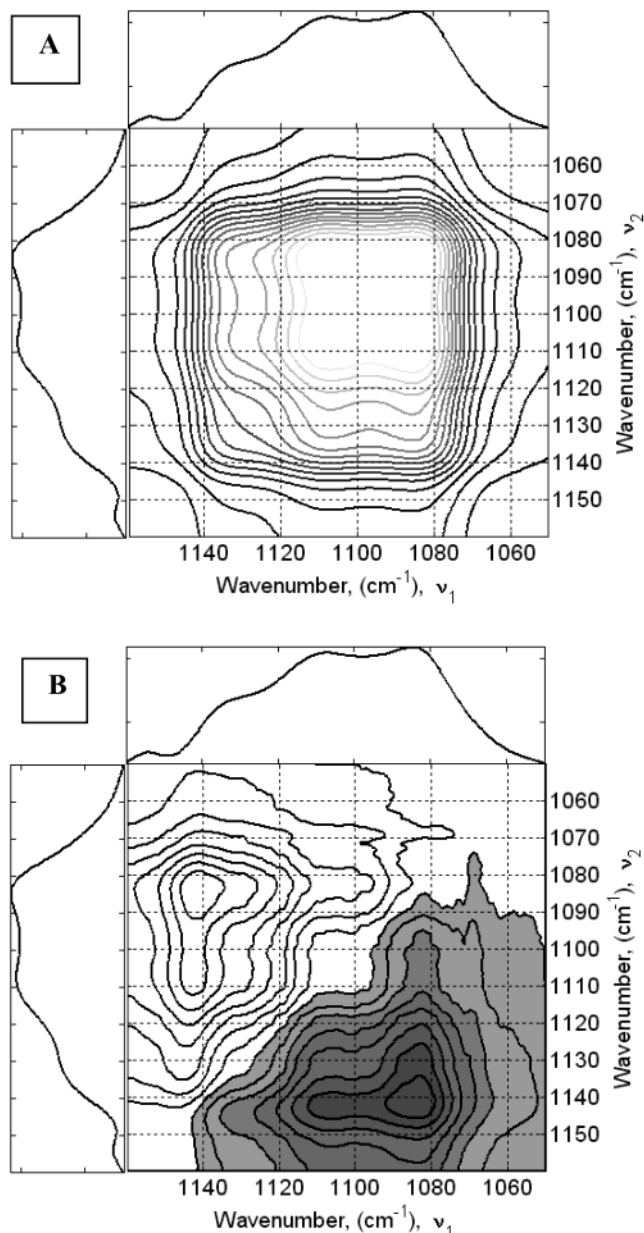


**Figure 15.** Synchronous (A) and asynchronous (B) contour plots of PS/PVME blends with high PS content in the C–O–C ether mode region of PVME.

spectra, of course, and has been commented on in previous work.<sup>3–5</sup>

A region where there are more interesting results is where C–O–C ether stretching modes of PVME appear, near 1100  $\text{cm}^{-1}$ . Synchronous and asynchronous plots obtained from high PS content blends are shown in Figure 15. The synchronous plots are again not very rewarding because of the overlap of the three or four bands that contribute to this band envelope. The asynchronous plots show that the band near 1080  $\text{cm}^{-1}$  has a different concentration dependence than the band near 1135  $\text{cm}^{-1}$ , however. The normal-coordinate calculations of Snyder and Zerbi<sup>14</sup> on model ethers indicated that the 1080  $\text{cm}^{-1}$  mode is predominantly associated with the C–O stretch of the ether group, while the 1135  $\text{cm}^{-1}$  band is predominantly a methyl CH bending mode.

Previous work has led to the suggestion that the lone pair electrons of the PVME ether group interact with

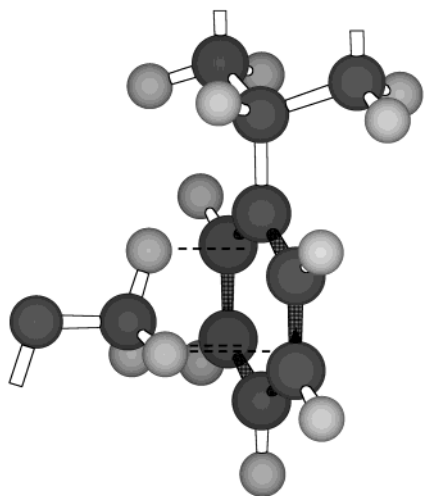


**Figure 16.** Schematic of a  $\text{CH}_3$  group of PVME oriented against the face of an aromatic ring of PS.

the  $\pi$ -bonds of the polystyrene ring. However, since that work, published more than 20 years ago, there have been a number of studies that lead us to believe that it may be the methyl group that is involved. Aromatic rings readily form  $\pi$ -cation complexes<sup>15,16</sup> and are also capable of interacting with  $\text{CH}_3$  groups through the formation of a weak  $\text{CH}\cdots\pi$  hydrogen bond.<sup>17</sup> A  $\text{CH}_3$  group oriented against the face of an aromatic ring, as illustrated in Figure 16, could interact fairly strongly through the formation of three such hydrogen bonds. Unfortunately, this is only a suggestion we can make on the basis of the weight of work on interactions in general that have been recently reported in the literature. The use of correlation infrared spectroscopy indicates that the intensities of bands assigned to ether and  $\text{CH}_3$  groups do not change in the same fashion with concentration but provides no information on which of these is more likely to be involved in the interaction.

## Conclusions

In this study we have applied correlation infrared spectroscopy to a study of miscible blends. As in the preceding study of immiscible systems, a rotated cloverleaf-like pattern was obtained in many regions of the spectrum, characteristic of bandwidth changes or overall spectral profile changes as a function of concentration.

These features have previously been interpreted in terms of the detection of previously hidden bands, specific interactions, and conformational changes. It is shown here that these features correspond to lobes or points of inflection in the difference spectra used to generate the 2D plots. Frequency shifts also give a characteristic pattern that can be easily misinterpreted. Great care must be taken when applying this methodology to systems like polymer blends.

**Acknowledgment.** This material is based upon work supported by the National Science Foundation under Grant 0100818.

## Note Added after ASAP Posting

This article was released ASAP on June 25, 2003. The following changes have now been made: Table 1, footnote *a* was added to the column head; Figure 2, the label for part A was adjusted; Figure 4, the label for part B was adjusted; paragraph 17 of the Results and Discussion, sentence 3, " $\text{CH}\pi$ -hydrogen" was changed to " $\text{CH}\cdots\pi$  hydrogen". The correct version was posted on 09/15/2003.

## References and Notes

- (1) Huang, H.; Malkov, S.; Coleman, M. M.; Painter, P. C. *Macromolecules* **2003**, *36*, 8148.
- (2) Wellinghoff, S. T.; Koenig, J. L.; Baer, J. *Polym. Sci., Polym. Phys. Ed.* **1977**, *15*, 1913.
- (3) Garcia, D. J. *Polym. Sci., Polym. Phys. Ed.* **1984**, *22*, 1773.
- (4) Garcia, D. J. *Polym. Sci., Polym. Phys. Ed.* **1984**, *22*, 107.
- (5) Lu, F. J.; Benedelti, E.; Hsu, S. L. *Macromolecules* **1983**, *16*, 1525.
- (6) Nakashima, K.; Ren, Y.; Nishioka, T.; Tsubahara, N.; Noda, I.; Ozaki, Y. *J. Phys. Chem. B* **1999**, *103*, 6704.
- (7) Satkowski, M. M.; Grothans, J. T.; Dowrey, A. E.; Noda, I. In *Polymer Solutions Blends and Interfaces*; Noda, I., Rubingh, D. N., Eds.; Elsevier Science: Amsterdam, 1992; p 89.
- (8) Greike, A.; et al. *Biospectroscopy* **1996**, *2*, 341.
- (9) Czarnacki, M. A. *Appl. Spectrosc.* **1998**, *52*, 1883.
- (10) Czarnacki, M. A. *Appl. Spectrosc.* **2000**, *54*, 986.
- (11) Elmore, D. L.; et al. *Appl. Spectrosc.* **2000**, *54*, 956.
- (12) Morita, S.; et al. *Appl. Spectrosc.* **2002**, *56*, 502.
- (13) Noda, I. *Appl. Spectrosc.* **1993**, *47*, 1329.
- (14) Snyder, R. G.; Zerbi, G. *Spectrochim. Acta, Part A* **1967**, *23A*.
- (15) Ma, J. C.; Dougherty, D. A. *Chem. Rev.* **1997**, *97*, 1303.
- (16) Dougherty, D. A. *Science* **1996**, *271*, 163.
- (17) Nishio, M.; Umezawa, Y.; Hirota, M.; Takeuchi, Y. *Tetrahedron* **1995**, *51*, 8665.

MA0259463